

Experimental Simulations: A Summary

I. INTRODUCTION

THIS is a summary of the course Experimental Simulations taught by prof. Eitelberg at Delft University of Technology in the academic year 2010-2011. This summary is no official course material, it has been made by a student, all figures and much of the text was taken form the course documents. No plagiarism intended, this is just a summary.

II. SIMILARITY

This is all very well and concisely explained in the notes of lecture 1, have a look at those for the complete discussion.

There are a number of ways to scale an experiment in such a way as to obtain similarity:

- 1) Write down the governing equations, non-dimensionalize those and select the right parameters.
- 2) Write down relevant variables, perform dimensional analysis and obtain a reduced set of governing parameters. When possible, obtain governing equations.
- 3) Write down relevant phenomena, express those through the relevant variables and analyze the relevant orders of magnitude.

Combinations thereof:

- 1) Method of fractional analysis
- 2) Method of dimensional analysis
- 3) Method of differential equation

Fractional Analysis

Inertia	$\left \begin{array}{l} F_I \propto U \frac{\partial u}{\partial x} \propto \frac{u^2}{L} \left[\frac{m}{s^2} \right] \\ F_p \propto \frac{1}{\rho} \frac{\partial p}{\partial x} \propto \frac{p}{\rho L} \left[\frac{Pa}{kg} \frac{m^3}{m} = \frac{m}{s^2} \right] \\ F_F \propto \frac{1}{\rho} \mu \frac{\partial^2 u}{\partial x^2} \propto \frac{\mu}{\rho} \frac{u}{L^2} \left[\frac{m}{s^2} \right] \\ F_G \propto g \left[\frac{m}{s^2} \right] \\ F_c \propto \frac{1}{\rho} \frac{\sigma}{L^2} \end{array} \right $
Pressure	
Friction	
Gravity	
(Free surface) capillarity	

TABLE I
FRACTIONS OF FORCES

Fractional analysis is not entirely complete:

- Energy equation not included
- Although forces were scaled with parameters describing magnitude, the inertia force is defined by acceleration ($u \frac{\partial u}{\partial x}$). This is zero in many cases (e.g. fully established (pipe flow), although the corresponding Reynolds number remains non-zero.

II-theorem: A physical relationship between some dimensional quantity and several dimensional governing parameters can be expressed as a relationship between a dimensionless parameter and several dimensionless products of the governing parameters. The number of dimensionless products is equal

Conduction	$\left \begin{array}{l} \dot{e}_{cd} \propto \frac{\lambda}{\rho} \frac{\partial^2 T}{\partial x^2} \propto \frac{\lambda \Delta T}{\rho L^2} \\ \dot{e}_{cv} \propto c_p u \frac{\lambda}{\rho} \frac{\partial T}{\partial x} \propto \frac{c_p u \Delta T}{L} \\ \dot{e}_{fr} \propto \nu \left(\frac{\partial u}{\partial y} \right)^2 \propto \frac{\nu u^2}{L^2} \\ \dot{e}_{ss} \propto \dot{Q} \\ (\dot{e}_{unsteady} \propto \frac{c_p \Delta T}{t}) \end{array} \right $
Convection	
Friction	
Sources/sinks	

TABLE III
FRACTIONS OF ENERGY FLUXES PER MASS ELEMENT

to the total number of governing parameters less the number of governing parameters with independent dimensions. \Rightarrow This can result in orders of magnitude reduction of evaluation effort.

III. WIND TUNNELS

Open circuit:

- Pro
 - Low construction effort
 - No cleaning
- Con
 - Frequency quality a function of environment prior to inlet
 - High energy requirement, flow accelerated form v=0
 - Noise radiation

Closed circuit:

- Pro
 - Flow quality determined by internal construction
 - Energy efficient
 - No environmental impact of operating noise
- Con
 - High cost of construction
 - Contamination settles in the circuit
 - Air cooling required

Classification of wind tunnels according to their velocity domain:

- Subsonic $M \ll 1$
- Transonic $M \approx 1$
- Supersonic $M > 1$
- Hypersonic $M \gg 1$

For all tunnels isentropic expansion through the nozzle is assumed:

$$\frac{T}{T_0} = \frac{1}{1 + \frac{\gamma-1}{2} M^2} \tag{1}$$

$$\frac{\rho}{\rho_0} = \frac{1}{\left(1 + \frac{\gamma-1}{2} M^2\right)^{\frac{1}{\gamma-1}}} \tag{2}$$

$$\frac{p}{p_0} = \frac{1}{\left(1 + \frac{\gamma-1}{2} M^2\right)^{\frac{\gamma}{\gamma-1}}} \tag{3}$$

$\frac{\text{pressure}}{\text{inertia}}$	$\frac{F_p}{F_I} = \frac{p}{\rho L} \frac{L}{u^2} = EU = \text{Euler number} = c_p/2$
$\frac{\text{inertia}}{\text{friction}}$	$\frac{F_I}{F_f} = \frac{u^2 \rho L^2}{L \mu u} = \frac{\rho u L}{\mu} = \frac{u L}{\nu} = Re$
$\frac{Ma}{Re}$	$\frac{Ma}{Re} = \frac{u a \Delta}{a u L} = \frac{\Delta}{L} = Kn \text{ (Knudsen number)} \text{ } (\Delta = \text{mean free path})$
$\frac{\text{inertia}}{\text{gravity}}$	$\frac{u^2}{L g} = Fr \text{ (Froude number)}$
$\frac{\text{inertia}}{\text{capillarity}}$	$\frac{u^2}{L} \frac{L^2 \rho}{\sigma} = \rho \frac{u^2}{\sigma} L = We$

TABLE II
FOUR INDEPENDENT RATIOS BUILT FROM THE FRACTIONS OF FORCES

$\frac{\text{convection}}{\text{conduction}}$	$\frac{\dot{e}_{cv}}{\dot{e}_{cd}} \propto \frac{c_p u \Delta T}{L} \frac{\rho L^2}{\lambda \Delta T} = \frac{c_p \rho u L}{\lambda} = \frac{u L}{\frac{\lambda}{\rho c}} = \frac{L}{k} = Pe = \text{Peclet number}$
$\frac{\text{friction}}{\text{convection}}$	$\frac{\dot{e}_{fr}}{\dot{e}_{cv}} \propto \frac{\nu^2}{L^2} \frac{L}{c_p u \Delta T} = \frac{1}{Re} \frac{u^2}{c_p \Delta T} = \frac{1}{Re} \cdot Ec \text{ (Eckert number)}$
$\frac{\text{unsteady}}{\text{conduction}}$	$\frac{\dot{e}_{unsteady}}{\dot{e}_{cd}} \propto \frac{c_p \Delta T}{t} \frac{\rho L^2}{\lambda \Delta T} = \frac{c_p \rho L^2}{\lambda t} = \frac{L^2}{kt} = Fo \text{ (Fourier number)}$
$\frac{\text{source/sink}}{\text{unsteady}}$	$\frac{\dot{e}_{ss}}{\dot{e}_{unsteady}} = \frac{\dot{Q} t}{c_p \Delta T} = \frac{Q}{c_p \Delta T} = Da \text{ (Damkohler number)}$

TABLE IV
INDEPENDENT FORM RATIOS WITH FRACTIONS OF ENERGY FLUXES (PER MASS ELEMENT

Energy transport equation	$c_p \frac{dT}{dt} = c_p \frac{\partial T}{\partial t} + c_p \left(u \frac{\partial T}{\partial x} + v \frac{\partial T}{\partial y} + w \frac{\partial T}{\partial z} \right) = \frac{1}{\rho} \nabla \cdot (\lambda \nabla T) + \frac{1}{\rho} \Phi + \dot{e}_{ss} + \dot{e}_{rd}$
Conservation of mass	
Conservation of momentum	
	$\frac{\partial u}{\partial x} + \frac{\partial v}{\partial y} = 0$ $u \frac{\partial u}{\partial x} + v \frac{\partial u}{\partial y} = -\frac{1}{\rho} \frac{\partial p}{\partial x} + \nu \nabla^2 u$ $u \frac{\partial v}{\partial x} + v \frac{\partial v}{\partial y} = -\frac{1}{\rho} \frac{\partial p}{\partial y} + \nu \nabla^2 v$

TABLE V
SOME USEFUL DIFFERENTIAL EQUATIONS

For finite angle of attack and $M < 1$:

$$C_L = \frac{2\pi\alpha}{\sqrt{1-M_\infty^2}} \cdot \frac{1}{1 + \frac{2}{\sigma\sqrt{1-M^2}}} \quad (4)$$

The first term in eq. 4 describes the influence of the Mach number on the lift coefficient at infinite aspect ratio, the second term is the correction for finite aspect ratio. This means that the Mach number influence in profile testing is not negligible, even at low compressibility. An increase in Mach number is equivalent to a reduction in span width. Thus it is preferable to obtain the Reynolds number independently of the Mach number variation.

For supersonic wind tunnels eq. 5 is very useful as it show that the Mach number obtained is only a function of the area ratio.

$$\left(\frac{A}{A^*} \right)^2 = \frac{1}{M^2} \left[\frac{2}{\gamma+1} \left(1 + \frac{\gamma-1}{2} M^2 \right) \right]^{\frac{\gamma+1}{\gamma-1}} \quad (5)$$

Now to determine the maximal velocity of a supersonic wind tunnel start out with the compressible formulation of the Bernoulli equation (conservation of momentum in a steam tube) neglecting gravity:

$$\frac{u^2}{2} + \frac{\gamma}{\gamma-1} \frac{p}{\rho} = \frac{u^2}{2} + \frac{a^2}{\gamma-1} = \text{const.} \quad (6)$$

and accelerating from rest:

$$\frac{a_0^2}{\gamma-1} = \frac{u^2}{2} + \frac{a^2}{\gamma-1} \quad (7)$$

$$\Rightarrow u_{max} = a_0 \sqrt{\frac{2}{\gamma-1}} \quad (8)$$

The power required for a continuous tunnel can be estimated from the total energy balance:

$$P = \dot{E} = \left(e + \frac{1}{2} u^2 \right) \dot{m} = \left(e + \frac{1}{2} u^2 \right) \rho u A \rightarrow \dot{E} \propto u^3 \quad (9)$$

First approximation for low speed tunnels:

$$\frac{P}{A} \approx \frac{1}{2} \rho u^3 \quad (10)$$

Sonic conditions in the throat (for air):

$$\frac{T^*}{T_0} = \frac{2}{\gamma+1} \approx 0.833 \quad (11)$$

$$\frac{\rho^*}{\rho_0} = \left(\frac{2}{\gamma+1} \right)^{\frac{1}{\gamma-1}} \approx 0.634 \quad (12)$$

$$\frac{p^*}{p_0} = \left(\frac{2}{\gamma+1} \right)^{\frac{\gamma}{\gamma-1}} \approx 0.528 \quad (13)$$

For blow down wind tunnels:

$$\frac{a^*}{a_0} = \sqrt{\frac{T^*}{T_0}} \approx 0.91 \quad (14)$$

The characteristic time of spreading of information is $\frac{D}{a_0}$. The characteristic time scales with the inverse of the mass flux and is proportional to the mass:

$$\frac{\frac{D}{a_0}}{\frac{\rho_0 D^3}{\rho^* u^* A^*}} \propto \frac{A}{D^2} \ll 1 \quad (15)$$

Under these conditions, with sufficient pressure ratio, the exit Mach number will remain constant, although the Reynolds number will not. If $\frac{A}{D^2} \ll 1$ is not fulfilled, or if there are multiple scales to be considered, wave propagation has to be considered.

IV. SIMULATION OF PROPULSION INTEGRATION EFFECTS

Interference effects from engine installation can result from:

- Geometrical elements such as cowl (extra surface and cross sectional area), pylon (inlet spillage) and jet interference (for example with high-lift devices)
- Wing pylon junction leading to loss of lift (less circulation at the wing)
- Junction flow
- Channel flow and fan exhaust interactions
- Jet induced flow/separation
- In case of wing mounted props, swirl in slipstream affects lift distribution

1) Installation effect: $F_{inst} = F_{powered} - F_{clean}$.

2) Power effect: $F_{power} = F_{powered\ at\ thrust} - F_{powered\ at\ ground\ idle}$.

3) Jet interference: $F_{jet} = F_{powered\ at\ thrust} - F_{powered\ at\ flight\ idle}$.

Engine simulators:

- TFN: Trough Flow Nacelle (aerodynamic shape that corresponds to the outer shell of the engine cowling and provides acceleration inside the hollow inner contour).
- TPS: Turbine Powered Simulators (compressed air drives a turbine which in turn drives the compressor, RPM up to 40000, mechanical operation needs to be monitored continuously).

Gross thrust of TPS is the sum of the thrust contribution of the fan and turbine:

$$X_G = c_{v,FN} \dot{m}_F V_{F,id} + c_{v,CN} \dot{m}_C V_{C,id} \quad (16)$$

with:

- $c_{v,FN}$ = fan nozzle velocity coefficient is obtained from calibration, the second one for the core nozzle
- $c_{v,CN}$ = the core nozzle velocity coefficient is supplied by the turbine manufacturer.
- the mass fluxes \dot{m}_F and \dot{m}_C are obtained from total pressure and temperature measurements in the calibration tank and the TPS supply line respectively.
- velocities $V_{F,id}$ and $V_{C,id}$ are obtained from the operational monitoring pressure and temperature data in the fan and core turbine exit planes. These velocities are calculated assuming isentropic expansion.

The fan nozzle velocity coefficient is determined from the total force and the thermodynamic property measurements in the calibration tank:

$$c_{v,FV} = \frac{X_F}{\dot{m} V_{F,id}} \quad (17)$$

$$X_F = X_G - c_{v,C} \dot{m}_C V_{C,id} \quad (18)$$

In order to obtain the net thrust, the inlet ram ($\dot{m} u_\infty$) needs to be subtracted from the gross thrust.

V. DESIGN OF EXPERIMENTS

Why “design” an experiment?

- It permits to answer questions with the smallest allocation of resources. – *Improves productivity.*
- It controls the probability of making improper inferences. – *Improves quality.*

The conventional way of testing is the “change factor at a time” approach (OFAT). But there are several problems with this approach:

- The total effect of a combination of parameter changes is not equal to the sum of the individual effects. For example test an aircraft with two flaps, first measure lift with one flap deployed, then with only the other flap deployed. $Lift_{total} \neq Lift_{flap1} + Lift_{flap2}$.
- It is difficult to find the optimal solution if the problem involves multiple variables each having a profound effect on the solution.
- It is almost impossible to see the effect of combinations of parameter changes.

To solve this problem you should not just change one parameter at a time, but change many factors at the same time to get a good image of the design space in the most efficient way possible (you should imagine the design space as an n-dimensional space with the n dimensions corresponding the n variables that influence the solution).

Statistical principles

Central limit theorem: *The sum of a large number of independent and identically distributed random variables will have an approximately normal distribution.*

Normal distribution:

$$P(x) = \frac{1}{\sqrt{2\pi\sigma^2}} e^{-\frac{(x-\mu)^2}{2\sigma^2}} \quad (19)$$

with:

Accuracy depends on two quantities:

- 1) σ quantifies random error (precision, repeatability and reproducibility)
- 2) β quantifies systematic error (bias).

- Poor repeatability means poor accuracy.
- Good repeatability does not necessarily mean good accuracy.

σ^2	Variance	$\sigma \approx \left[\frac{1}{N-1} \sum_{i=1}^N (X_i - \bar{X})^2 \right]^{1/2}$	$\sigma_{\bar{y}} = \frac{\sigma_y}{\sqrt{n}}$
σ	Standard deviation		
μ	Mean	$\mu \approx \bar{X} = \frac{1}{N} \sum_{i=1}^N X_i$	
	$[-\sigma, \sigma] \approx 68\%$		
	$[-2\sigma, 2\sigma] \approx 95\%$		
	$[-3\sigma, 3\sigma] \approx 99.7\%$		
	$[-\infty, \infty] = 100\%$		

TABLE VI
STOCHASTIC SYMBOLS

- Good accuracy means good repeatability

By using a Taylor series of the $f(X + \Delta X)$ one can derive the error propagation equation (eq. 21):

$$\sigma_f^2 = \sum_{i=1}^n \left(\frac{\partial f}{\partial x_i} \right)^2 \sigma_{x_i}^2 \quad (20)$$

$$U_f^2 = \sum_{i=1}^n \left(\frac{\partial f}{\partial x_i} \right)^2 U_{x_i}^2 \quad (21)$$

Quality assurance

Quality assurance techniques:

- Replication (allows you to get a better estimate of the standard deviation for example)
- Randomization (guards against bias errors)
- Blocking (used to correct for bias shifts)
- Interference space site selection

Factorial designs

- “Full factorial designs” feature all combinations of every level of every independent variable (or “factor”).
- They are a good way to examine main effects and interaction effects of many variables.
 - Main effect: Response change due to change in the level of an individual variable (like the change in drag due to the change in angle of attack).
 - Interaction effect: Change in main effect due to a change in some other variable (like the change in angle-of-attack effect on drag due to a change in Mach number).

Factorial designs are more efficient than OFAT designs and they are better at finding the interaction effects. One can use factorial designs to “screen” an experiment in order to find important variables among a large number of variables.

If you half the number of test point from your fractional design, you end up with a half-fractional fractional design (in a similar way you can get a quarter-fractional fractional design).

In the half-fractional design:

- Main effects are aliased with 5-way interactions.
- 2-way interactions are aliased with 4-way interactions.
- 3-way interactions are aliased with 3-way interactions.
- In general, n-way interactions are aliased with m-way interactions where $n + m = 6$.

In the quarter-fractional design:

- Main effects are aliased with 4-way interactions.
- 2-way interactions are aliased with 3-way interactions.
- In general, n-way interactions are aliased with m-way interactions, where $n + m = 6 - 1 = 5$.

Run Number	Variable						Block
	A	B	C	D	E	F	
1	-	-	-	-	-	-	I
2	-	-	-	-	-	+	II
3	-	-	-	-	+	-	II
4	-	-	-	-	+	+	I
5	-	-	-	-	+	-	II
6	-	-	-	-	+	+	I
7	-	-	-	-	+	+	I
8	-	-	-	-	+	+	II
.
.
.
63	+	+	+	+	+	-	II
64	+	+	+	+	+	+	I

Fig. 1. Example of the design of an experiment

Run Number	Main Effects						Two-factor Interactions				Five-factor Interactions				Six-Factor Interaction	
	A	B	C	D	E	F	BF	CF	DF	EF	...	ABCDE	ABCDF	ABCEF	ABCDEF	
1	-	-	-	-	-	-	...	+	+	+	+	...	-	-	-	+
4	-	-	-	-	+	+	...	-	-	-	-	...	+	+	-	+
6	-	-	-	-	+	-	...	+	+	-	-	...	+	-	+	+
7	-	-	-	-	+	+	...	+	+	-	-	...	-	+	-	+
10	-	-	-	-	+	-	...	+	+	-	-	...	-	-	-	+
11	-	-	-	-	+	+	...	+	+	-	-	...	-	+	-	+
13	-	-	-	-	+	-	...	+	+	-	-	...	-	-	-	+
16	-	-	-	-	+	+	...	+	+	-	-	...	+	+	-	+
.
.
.
64	+	+	+	+	+	+	...	+	+	+	+	...	+	+	+	+

Fig. 2. Note the F effect has the same signs as the ABCDE effect, we say the F effect is aliased with the ABCDE effect.

While the benefits of factorial designs include “hidden replication”, high efficiency (small volume of data) and have a wide inductive basis, there are also drawbacks to this technique. It is only suitable for linear models with interaction terms and is only suitable for factors with two levels.

Optimal designs

One can approximate a function by a Taylor expansion of degree d . The minimum volume of data necessary to fit this d^{th} order polynomial in k factors is:

$$p = \frac{(p+k)}{dk} \quad (22)$$

By expanding the function $Y = Xb$ as a Taylor expansion we in fact get $Y = Xb + \epsilon$. Now define L as $L = \sum_{i=1}^n \epsilon^2 \Rightarrow L = Y'Y - 2b'X'Y - b'X'Xb$ now find the b that minimizes L : $\frac{\partial L}{\partial b} = -2X'Y - 2X'Xb = 0; \Rightarrow \hat{b} = (X'X)^{-1}X'Y$ and $\Rightarrow \hat{Y} = X\hat{b} = (X(X'X)^{-1}X')Y$. Now we can either minimize $\|(X'X)^{-1}\|$, this is called a D-optimization or we can minimize the integral $diag(X(X'X)^{-1}X')$ this is called I-optimization. Note that factorial designs are D- and I-optimal.

The optimal number of points can be computed to be:

$$n = p(z_\alpha + z_\beta)^2 \frac{\sigma^2}{\delta^2} \quad (23)$$

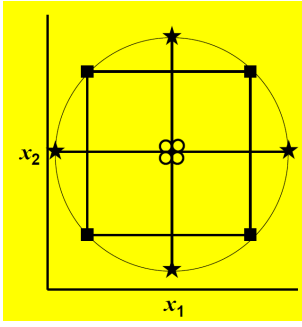


Fig. 3. An I-optimal design

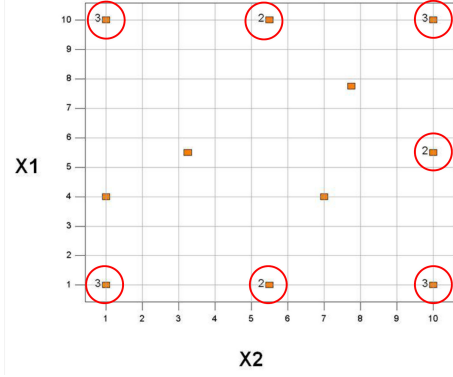


Fig. 4. A D-optimal design.

VI. ACOUSTICS

Acoustic waves, 1-D description:

$$\frac{\partial^2 p}{\partial x^2} - \frac{1}{c^2} \frac{\partial^2 p}{\partial t^2} = 0 \quad (24)$$

$$\text{with } c^2 = \gamma RTa \text{ (} c \text{ is the speed of sound)} \quad (25)$$

$$\text{solution : } p = f_1(ct - x) + f_2(ct + x) \quad (26)$$

$$\text{for vibrating source :} \quad (27)$$

$$p = A_1 \sin(\omega t - kx + \phi_1) + A_2 \sin(\omega t + kx + \phi_2) \quad (28)$$

And in eq. 28 ω is the frequency of the harmonic oscillation, $k = \omega/c = 2\pi/\lambda$ is the wave number and λ is the wavelength.

Characteristic specific acoustic impedance:

$$R = \rho c \quad (29)$$

$$\text{for air : } R = 1.2 \left[\frac{\text{kg}}{\text{m}^3} \right] 340 \left[\frac{\text{m}}{\text{s}} \right] = 415 \left[\frac{\text{kg}}{\text{m}^2} \right] \quad (30)$$

Sound intensity:

$$I = \frac{p_{rms}^2}{R} \left[\frac{\text{W}}{\text{m}^2} \right] \quad (31)$$

And for the RMS value of a sinusoidal sound wave:

$$I = \frac{p^2}{2R} \quad (32)$$

Sound power: *the surface integral over a closed surface including the source within it.*

Radiated power is a function of its boundary conditions:

- Solid wall doubles the power of a dipole.
- Corner quadruples the power of a dipole.

Sound pressure level:

$$L_p = 20 \cdot \log_{10} \frac{p_{rms}}{p_{ref}} \text{ [dB]} \quad (33)$$

$$\text{with } p_{ref} = 20 \text{ [\mu Pa]} \quad (34)$$

Sound power level:

$$L_P = 20 \cdot \log_{10} \frac{P}{P_{ref}} \quad (35)$$

$$\text{with } P_{ref} = 10^{-12} \text{ [W]} \quad (36)$$

Note $80\text{dB} + 80\text{dB} = 83\text{dB}$.

Scaling

Acoustic power of a dipole scales as:

$$\frac{p^2}{(\rho_0 c_0^2)^2} \propto M^6 \quad (37)$$

Note that the fluctuating sound pressure p is scaled with a reference pressure ρc^2 .

For a compact subsonic jet (with characteristic wavelength in the order of $\lambda = c \cdot D/U$ with D the jet diameter) at low Mach number the scaling goes according to:

$$\frac{p^2}{(\rho_0 c_0^2)^2} \propto M^8 \quad (38)$$

In the case of scattering from an edge (where the wall stops):

$$\frac{p^2}{(\rho_0 c_0^2)^2} \propto M^5 \sin\left(\frac{\Theta_e}{2}\right) \quad (39)$$

Looking at the directional characteristics of Eq. 39, it is clear that the edge is the most efficient sound generator in the flow field.

Free turbulence is a less efficient sound generator than wall bounded turbulence, for measurement purposes the amplitude decay with the distance squared needs to be considered $(D/r)^2$.

Doppler frequency shift:

$$\omega_{shifted} = \frac{\omega}{1 - (w/c)} \quad (40)$$

With w being the velocity with which the wave from a single source is carried; ω frequency at which the wave is emitted (period $T = 2\pi/\omega$).

Measurement Devices

Microphones:

- capacitive: use capacity variation caused by deformation of pressure sensitive membrane isolated from a fixed metal electrode.
- resistive: variation in strain is measured, the membrane is attached to a fixed structure.

Typical data acquisition performance:

- 100 to 144 microphone channels
- 120 kHz sample frequency
- 30 seconds continuous acquisition

Phased microphone arrays in open jet test section:

- Advantages:
 - Testing hall around the Open Jet provides a semi-anechoic environment
 - Array can be used in parallel with classical far-field microphone measurements
- Disadvantages:
 - Serious disturbances due to shear layer (need for Amiet correction; strong coherence loss for $f > 20kHz$)
 - Long distances between model and array (limitations of the resolution for frequencies $\gg 15kHz$)
 - Quality of aerodynamic simulations in the Open Jet is lower than in closed test sections

Arrays in closed test sections:

- Advantages:
 - Significant data up to $50kHz$ (1/3 octave band) \rightarrow acceptable coherence loss for high frequencies.
 - Short distances between array and model \rightarrow high resolution.
 - No interferences with aerodynamic measurements \rightarrow array measurements carried out in parallel to aerodynamics.
 - No loss of aerodynamic simulation quality
- Challenges:
 - Test section is an acoustically hard wall environment \rightarrow standing waves, acoustic reflections on test section walls.
 - Array microphones exposed to boundary layer noise \rightarrow high sound pressure levels (SPL).
 - No combination with far-field microphone measurements.

Phased microphone arrays are successfully implemented as an efficient aeroacoustic measurement technique in DNW wind tunnels. Especially the Wall-Array techniques is a valuable tool which allows the combined investigation of aerodynamics and aeroacoustics. A challenge that remains is the transfer of array results to far-field data and absolute levels.

VII. WIND TUNNEL CORRECTIONS

First of all some symbols involved, go through the list and you will get a general idea of what is involved.

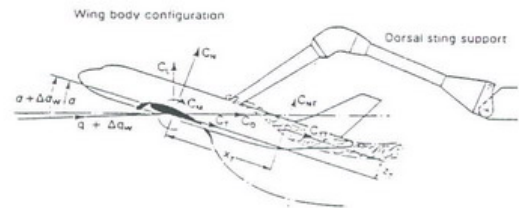
Support structures of the wind tunnel models always penetrate the so-called near field of the model flow. Therefore,

C	coefficient of load component
C_D	drag coefficient
C_L	lift coefficient
C_I	coefficient of interference load
C_M	pitching moment coefficient
C_N	normal force coefficient
C_{NT}	coefficient of normal force disturbance
C_{TI}	axial force coefficient
\bar{c}	mean aerodynamic chord
Δq_w	wing kinetic pressure disturbance
q	kinetic pressure
X_i	polynomial coefficients
X_T	axial distance
Z_T	normal distance
α	angle of attack
$\Delta\alpha_w$	wing angle of attack disturbance
σ	standard deviation

TABLE VIII
LIST OF SYMBOLS

support effects on aerodynamic coefficients, evaluated either by measurement or calculation, depend on the specific configuration of the model and model/support intersection. In Figure 5 seven different support arrangements are shown, all of these arrangements are needed to determine the support influences C_I incorporated in the measured load components C_i of each configuration. A linear combination of four different measurements define the support influences that are then used as correction terms to correct the measurements with a model supported by one of the three alternative sting arrangements.

A dorsal sting will induce a downwash effect on the wing, whereas a ventral sting will induce an upwash at the wing. The effects of the stings on drag are of the same order of magnitude but with a different sign. The pitching moment is most affected by a ventral or rear sting (certainly on models with horizontal stabilizer installed) because they induce a larger variation of the disturbance field of the support along the model tail.



$$\left(\frac{\partial C_L}{\partial \alpha} - C_D\right) \Delta \alpha_w - C_L \frac{\Delta q_w}{q} - \cos \alpha C_{DT} - \sin \alpha C_{TT} - \Delta C_L \quad (5)$$

$$\left(\frac{\partial C_D}{\partial \alpha} - C_I\right) \Delta \alpha_w - C_D \frac{\Delta q_w}{q} + \sin \alpha C_{DT} + \cos \alpha C_{TT} - \Delta C_D \quad (6)$$

$$\frac{\partial C_M}{\partial \alpha} \Delta \alpha_w - C_M \frac{\Delta q_w}{q} - \frac{X_T}{c} C_{DT} + \frac{Z_T}{c} C_{TT} - \Delta C_M \quad (7)$$

$$\Delta \alpha_w - X_1 - X_2 \alpha + X_3 \alpha^2 \quad (8)$$

$$\frac{\Delta q_w}{q} - X_4 - X_5 \alpha + X_6 \alpha^2$$

$$C_{DT} - X_7 - X_8 \alpha + X_9 \left(\frac{C_L}{\alpha}\right)$$

$$C_{TT} - X_{10} - X_{11} \alpha + X_{12} \left(\frac{C_N}{\alpha}\right)$$

Fig. 6. Analysis of support effects on the longitudinal coefficients

So what is basically done to determine the influences of

SPL_{max}	$\geq 130dB$	due to boundary layer noise
Low self noise level L_{noise}	$< 20dB$	for high frequency signals
High sensitivity S	$> 10mV/Pa$	sufficient signal to noise ratio
Broad frequency range f_{range}	$\leq 100Hz$ to $\geq 40kHz$	for scale models

TABLE VII
MICROPHONE REQUIREMENTS FOR APPLICATIONS IN WIND TUNNELS

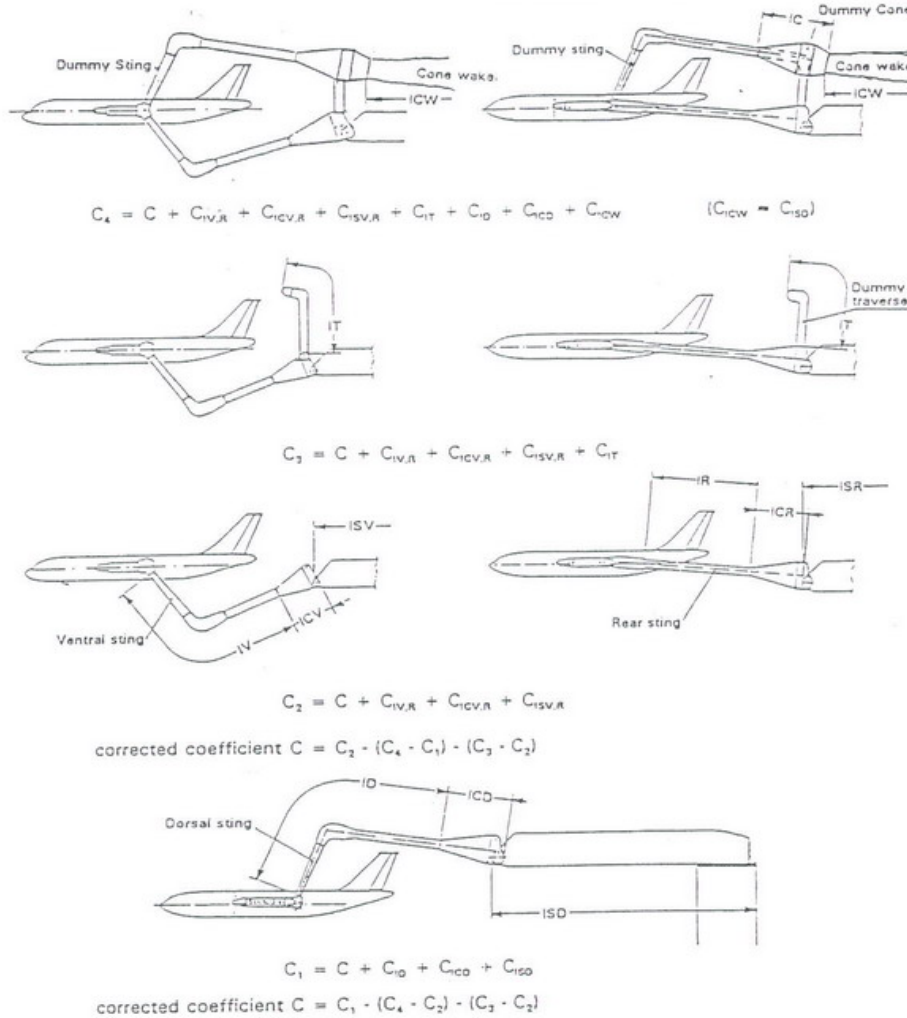


Fig. 5. Support arrangements for interference measurements [Source [1]].

stings and support structures is to do measurements with different setups (one with ventral and one with dorsal sting for example) and then add or subtract these data obtained in a smart way to deduce the influence every element of the support structure has. These influences can of course also be modeled and there are two main interface mechanism that are to be taken into account [1]:

- The wing of the model is only affected by far field support influences represented by a rotation $\Delta\alpha_w$ and a change of the kinetic pressure Δq_W of the undisturbed flow. In this sense $\Delta\alpha_W$ and Δq_W are wing averaged values.
- The fuselage model is affected by far field influences in combination with near field effects as a consequence of the inhomogeneous pressure field induced at the model

by the support volumes which are moving relative to the model and to the test section walls during an angle of attack polar. The far field effect will result in an axial buoyancy load on the fuselage tail. The wake of the dorsal sting affects the vertical tail and the trace of the horseshoe vortex around the sting/fuselage intersection influences the fuselage aft part.

Some conclusions from [1]:

- The near field dependent contributions to the support corrections are small compared to the far field effects.
- The far field effects might be determined using support dependent flow direction and kinetic pressure disturbances relevant for wing and fuselage.
- The far field disturbances may be evaluated from classical

interference measurements with the model presented or without the model by probe measurements.

REFERENCES

- [1] Eckert D., *A semi-analytic method to correct for support effects on wind tunnel models*, German-Dutch Wind Tunnel (DNW)
- [2] Dr. Ir. Bergmann, R., *Design of Experiment*, lecture at Delft University of Technology
- [3] prof.dr.ing. Eiterlberg, G., *Lecture notes and additional course material*